Radiative and transport properties of ions in strongly coupled plasmas

David B. Boercker and Carlos A. Iglesias
Lawrence Livermore National Laboratory, University of California, Livermore, California 94550

James W. Dufty
Department of Physics, University of Florida, Gainesville, Florida 32611
(Received 27 March 1987)

A simple model is proposed for the dynamical effects of a strongly coupled plasma on the center-of-mass and internal coordinates of an ion. The ion is coupled to the plasma through monopole and dipole interactions. The radiative and transport properties of the ion are intimately related since both are governed by the electric microfield at the ion. A unified description of both types of properties is obtained by a formulation focused on the dynamics of the electric microfield. The velocity autocorrelation function, self-structure factor, and electric field correlation function are all in good agreement with computer simulation results, even for strongly coupled plasmas. The effects of perturbing ion motion on Lyman-α and Lyman-β spectral line profiles are calculated. Again, good agreement with computer-simulation results is obtained.

I. INTRODUCTION

The motion of a point ion in a plasma is determined by the net instantaneous Coulomb force exerted on it by the plasma. Similarly, for an ion with a dipole moment, both center of mass and internal degrees of freedom couple to the plasma only through the total force. These observations suggest that an appropriate formulation of the radiative and transport properties of an ion in a strongly coupled plasma could be given in terms of a limited set of variables consisting of all degrees of freedom for the ion, and *only* the electric field for the plasma. This point of view is motivated by the fact that a detailed dynamical description in terms of particle trajectories and cross sections is not practical in general for a strongly coupled plasma. Instead, an approach based on collective properties (like the total field) is both more relevant and practical. The objective here is to propose such a model that is suitable for calculation of both the center-of-mass motion (transport) and the radiative properties. The self-consistency of these two types of properties allows important relationships to be imposed between self-diffusion and the spectral line shapes.

The motivations for our model come from existing methods in plasma line broadening for neutral atoms, and transport theory for neutral fluids. The idea of describing the interaction of the plasma and an atomic dipole by an effective stochastic field has been proposed earlier by Brissaud and Frisch.[1] Subsequent applications to the calculation of line shapes from neutral atoms have been quite successful.[2] Although the stochastic process used was highly idealized, a proper formulation of this approach based in statistical mechanics has been given.[3] An advantage of this general formulation is that it is easily extended to charged radiators, and approximation methods from transport theory[4] can be applied.

Recent interest in spectral line broadening has shifted to experiments on hot, dense laser-produced plasmas.[5] Such plasmas can be strongly coupled and the charge and mass of the radiating ion can be very different from those for the perturbing ions. Under these conditions it is important for the theoretical description to be general, simple (practical), and accurate to the extent of including all qualitative features. In this spirit, the approximations inherent in the model presented here preserve the most important physical properties of the exact formulation, while allowing explicit calculations. Furthermore, these approximations imply no limitation on the plasma state, so the results should apply even for strong coupling. Ultimately, all parameters of the model can be computed from the pair correlation function. To check the accuracy of these approximations the electric field autocorrelation function is calculated for a one-component plasma at coupling strengths $\Gamma = 1$, 2, and 5. Comparison with computer simulation[6] results shows good agreement. The model preserves the relationship of electric microfield and ion velocity; so the velocity autocorrelation function is also well described. For similar reasons, the dynamic structure factor has the correct dependence on the velocity autocorrelation function in the Gaussian limit and consequently also agrees well with computer simulation results.[7]

Plasma broadening of spectral lines arises from interaction of the radiator with both electrons and ions of the plasma. Most theories in the past have assumed that the ions are static during the relevant radiation times.[8] However, this assumption can lead to significant disagreement with experimental results for neutral hydrogen.[9] Recently, computer simulations have been performed to study the effects of ion dynamics on spectral line shapes of highly charged hydrogenic radiators[10] and large effects due to ion dynamics are also observed near line center. We apply the simplest version of our model to calculate the Lyman-α and Lyman-β lines, and find good agreement with the simulations. The relationship to other theoretical approaches[11] is discussed briefly.

II. ELECTRIC FIELD AND CENTER-OF-MASS DYNAMICS

Most physical properties of an ion in a plasma can be expressed in terms of time correlation functions of the form

$$C_{AB}(t)\equiv V^{-1}\langle A^{\dagger}B(t)\rangle \ , \tag{2.1}$$

where V is the volume of the system and the brackets denote an equilibrium average over degrees of freedom for the plasma plus ion. To simplify the discussion, the plasma is taken to be a classical one-component system (OCP) of ions with charge Z_0 and mass m_0 in a neutralizing background. To distinguish the impurity ion, of charge Z and mass m, it will be referred to as the radiator. The radiator is assumed to interact with the plasma only through its monopole and dipole moments. Consequently, attention is restricted to observables A and B that are functions of the center-of-mass and internal coordinates of the radiator, and the total ion electric microfield at the radiator,

$$A=A(a,\mathbf{p})e^{i\mathbf{k}\cdot\mathbf{r}},\quad B=B(a,\mathbf{p})e^{i\mathbf{k}\cdot\mathbf{r}} \ . \tag{2.2}$$

Here, a denotes collectively all internal degrees of freedom and $(\mathbf{r},\mathbf{p})$ denote the center-of-mass position and momentum. Translational invariance of the equilibrium ensemble and bilinearity of $C_{AB}(t)$ allows construction of correlation functions for variables with more general $\mathbf{r}$ dependence from those considered here, by superposition. The average in Eq. (2.1) can be performed in two steps: first an average over plasma degrees of freedom, followed by an average over the radiator degrees of freedom,

$$C_{AB}(t)=\operatorname*{Tr}_a \int d\mathbf{p}\, A^{\dagger}(a,\mathbf{p})f(a,\mathbf{p})B(a,\mathbf{p};\mathbf{k};t) \ . \tag{2.3}$$

The average is taken over internal and center-of-mass states of the radiator, and $f(a,\mathbf{p})$ is the reduced density operator for these variables. The effective time dependence of the radiator in the presence of the plasma is described by $B(a,\mathbf{p};\mathbf{k};t)$. The determination of this average dynamics is the central problem since its knowledge reduces the calculation to consideration of only the degrees of freedom of the radiator. Since the coupling of the radiator to the plasma is entirely through the electric field $\mathbf{E}$, the average dynamics of $B(a,\mathbf{p};\mathbf{k};t)$ is decomposed further into an average over plasma states with a fixed value $\mathbf{E}=\boldsymbol{\varepsilon}$, followed by an average over the distribution of values, $\boldsymbol{\varepsilon}$,

$$B(a,\mathbf{p};\mathbf{k};t)=\int d\boldsymbol{\varepsilon}\, Q(\boldsymbol{\varepsilon})B(a,\mathbf{p},\boldsymbol{\varepsilon};t) \ , \tag{2.4}$$

where $Q(\boldsymbol{\varepsilon})$ is the electric microfield distribution for the probability density of electric field values [the $\mathbf{k}$ dependence on the right-hand side of (2.4) has been suppressed for simplicity]. The objective now is to describe the dynamics of the radiator entirely through the "relevant" variables $(a,\mathbf{p},\boldsymbol{\varepsilon})$.

An exact equation for $B(a,\mathbf{p},\boldsymbol{\varepsilon},t)$ in the chosen variables can be obtained from Zwanzig's projection operator method,[12] as outlined in Appendix A,

$$\left[\frac{\partial}{\partial t}-L(a,\boldsymbol{\varepsilon})+\frac{i\mathbf{k}\cdot\mathbf{p}}{m}-eZ\boldsymbol{\varepsilon}\cdot\boldsymbol{\nabla}_p-p_i\sigma_{ij}(\boldsymbol{\varepsilon})\frac{\partial}{\partial\varepsilon_j}\right]B(t) = \int_0^t d\tau\, M(t-\tau)B(\tau) \ , \tag{2.5}$$

where repeated indexes imply a summation. The second, third, and fourth terms on the left-hand side represent internal and center-of-mass motion of an isolated radiator in a force field, $eZ\boldsymbol{\varepsilon}$. Next, $\sigma_{ij}(\boldsymbol{\varepsilon})$ is the average field gradient tensor, giving the average or "mean-field" rate of change of the force. The operator $M(t)$ on the right-hand side describes dynamical transitions between different field values. This term vanishes at $t=0$, so the left-hand side can be interpreted as describing the exact short-time dynamics. The plasma and radiator center-of-mass variables are taken to be classical, although the internal coordinates are treated quantum mechanically. The model considered here results from an approximation for $M(t)$. To define this model and to simplify the following calculations, it is useful to introduce a Laplace transform by

$$\bar{B}(a,\mathbf{p},\boldsymbol{\varepsilon};\omega)=\int_0^{\infty} dt\, e^{-i\omega t}B(a,\mathbf{p},\boldsymbol{\varepsilon};t) \ . \tag{2.6}$$

A scalar product is introduced also by

$$(X,Y)\equiv\operatorname*{Tr}_a\int d\mathbf{p}\int d\boldsymbol{\varepsilon}\, X^{\dagger}(a,\mathbf{p},\boldsymbol{\varepsilon})f(a,\mathbf{p},\boldsymbol{\varepsilon})Y(a,\mathbf{p},\boldsymbol{\varepsilon}) \ , \tag{2.7}$$
$$f(a,\mathbf{p},\boldsymbol{\varepsilon})=f(a,\mathbf{p})Q(\boldsymbol{\varepsilon}) \ .$$

The Laplace-transformed correlation function can then be written in the compact form

$$\bar{C}_{AB}(\mathbf{k},\omega)=(A,\mathcal{R}B) \ ,$$
$$\mathcal{R}^{-1}\equiv i\omega+\frac{i\mathbf{k}\cdot\mathbf{p}}{m}-L(a,\boldsymbol{\varepsilon})-\mathcal{L}-\bar{M}(\omega) \ , \tag{2.8}$$
$$\mathcal{L}\equiv eZ\boldsymbol{\varepsilon}\cdot\boldsymbol{\nabla}_p+p_i\sigma_{ij}(\boldsymbol{\varepsilon})\frac{\partial}{\partial\varepsilon_j} \ .$$

Several constraints on the operators $\mathcal{L}$ and $\bar{M}$ are imposed by conservation of probability, stationarity, and the relationship of $\mathbf{p}$ to $\mathbf{E}$:

$$\mathcal{L}\mathbf{p}=Ze\mathbf{E} \ ,$$
$$(X,[\mathcal{L}+L(a,\boldsymbol{\varepsilon})Y])=-([\mathcal{L}+L(a,\boldsymbol{\varepsilon})]X,Y) \ , \tag{2.9}$$
$$[\mathcal{L}+L(a,\boldsymbol{\varepsilon})]f(a,\mathbf{p},\boldsymbol{\varepsilon})=0$$

and

$$(W,\bar{M}X)=0=(X,\bar{M}W) \ ,$$
$$\lim_{\omega\to\infty}\bar{M}(\omega)=0 \ . \tag{2.10}$$

In these equations X and Y are arbitrary, but W is independent of $\boldsymbol{\varepsilon}$. The proof of Eqs. (2.9) and (2.10) is also given in Appendix A. There are methods to construct models of operators such as $\bar{M}$ that have been very successful in the kinetic theory of gases.[13] The simplest such model consistent with the properties of (2.10) is[14]

$$\bar{M}Y(\mathbf{p},\boldsymbol{\varepsilon})=-\nu(\Delta\omega)\left[Y(\mathbf{p},\boldsymbol{\varepsilon})-\int d\boldsymbol{\varepsilon}'\,Q(\boldsymbol{\varepsilon}')Y(\mathbf{p},\boldsymbol{\varepsilon}')\right] \ , \tag{2.11}$$
$$\Delta\omega\equiv\omega+\frac{\mathbf{k}\cdot\mathbf{p}}{m}+iL(a,\boldsymbol{\varepsilon}=0) \ .$$

A possible dependence of Y on internal degrees of freedom and the transform variables $(\mathbf{k},\omega)$ have been left implicit. The function $\nu(\Delta\omega)$ is a parameter of the model that is arbitrary at this point, except for the constraints

$$\lim_{\omega\to\infty}\nu(\Delta\omega)=0, \quad \nu^{\dagger}(\Delta\omega)=\nu(-\Delta\omega) . \tag{2.12}$$

It is straightforward to verify that this model preserves all of the fundamental symmetries of the correlation functions resulting from rotation, translation, time reversal, and stationarity.

With this model, the calculation of the correlation functions is essentially reduced to quadratures, in the sense that the result can be expressed in terms of the solution to the isolated radiator equations, (2.5) with $M=0$. This is proved in Appendix B. The simplest case is the class of correlation functions for which A and B are independent of **E**,

$$\bar{C}_{AB}(\mathbf{k},\omega)=\operatorname{Tr}_a\int d\mathbf{p}\, A^{\dagger}(a,\mathbf{p})f(a,\mathbf{p})[1-G(\Delta\omega)\nu(\Delta\omega)]^{-1} \times G(\Delta\omega)B(a,\mathbf{p}) , \tag{2.13}$$

where $G(\Delta\omega)$ is an operator on functions of $\mathbf{p}$ and on internal coordinates, defined by,

$$\begin{aligned} G(\Delta\omega)&\equiv\int d\varepsilon\, Q(\varepsilon)R(\Delta\omega) ,\\ R(\Delta\omega)&=[i\Delta\omega-L_I(\varepsilon)+\nu(\Delta\omega)-\mathcal{L}]^{-1} ,\\ L_I(\varepsilon)&\equiv\frac{1}{i\hbar}[\cdot,\varepsilon\cdot\mathbf{d}] . \end{aligned} \tag{2.14}$$

Here the operator for the atomic internal degrees of freedom, $L(a,\varepsilon)$, has been separated into a part for the isolated atom, $L(a,\epsilon=0)$, and a part for its dipole interaction with the field, $L_I(\varepsilon)$. These results also provide a connection with the more usual kinetic-theory approaches to transport properties. To make this more explicit, (2.13) is written as

$$\bar{C}_{AB}(\mathbf{k},\omega)=\operatorname{Tr}_a\int d\mathbf{p}\, A^{\dagger}(a,\mathbf{p})f(a,\mathbf{p}) \times[i\Delta\omega+\Lambda(\Delta\omega)]^{-1}B(a,\mathbf{p}) , \tag{2.15}$$

$$[i\Delta\omega+\nu(\Delta\omega)+\Lambda(\Delta\omega)]^{-1}\equiv G(\Delta\omega) . \tag{2.16}$$

The operator $\Lambda(\Delta\omega)$ can be identified now as the collision operator of kinetic equations for a tagged particle with internal degrees of freedom. The difference here is its approximate representation, (2.16), in terms of the dynamics of the total force applied by the fluid rather than in terms of few-particle scattering operators. The expectation is that (2.16) will be suitable for strongly coupled systems where simultaneous many-body interactions are important. It is possible to show that the usual Fokker-Planck operator is recovered from (2.16) in the weak-coupling limit.

III. DETERMINATION OF PARAMETERS

The operator $\mathcal{L}$ describes the instantaneous changes in the plasma field, ε, due to the radiator. This operator vanishes for a neutral radiator since there is no direct coupling of the plasma and center-of-mass radiator variables in this limit. In contrast, $\nu(\Delta\omega)$ represents a rate of change of electric field values due to dynamics of plasma configurations, which occurs even for a neutral radiator. Generally, there is no simple or direct relationship of $\nu(\omega)$ to the transport properties of a neutral radiator but, for charged radiators, the operator $\mathcal{L}$ couples the center-of-mass motion to field fluctuations and the dissipative properties are directly related to $\nu(\Delta\omega)$. This relationship can be exploited to determine $\nu(\Delta\omega)$ as follows.

In the simplest case it is assumed that $\nu(\Delta\omega)$ is independent of the internal degrees of freedom and can be characterized by the momentum autocorrelation function for a point ion [i.e., $L(a,\varepsilon)=0$]. Equations (2.15) and (2.16) with $A=\mathbf{p}=B$ and $\mathbf{k}=0$ give

$$\begin{aligned} \bar{C}_{pp}(\omega)&=\int d\mathbf{p}\,\phi(p)\mathbf{p}\cdot[i\omega+\Lambda(\omega)]^{-1}\mathbf{p} ,\\ [i\omega+\nu(\omega)+\Lambda(\omega)]^{-1}&=\int d\varepsilon\, Q(\varepsilon)[i\omega+\nu(\omega)-\mathcal{L}]^{-1} , \end{aligned} \tag{3.1}$$

where $\phi(p)$ is the Maxwell-Boltzmann distribution. As expected, $\bar{C}_{pp}(\omega)$ is related to $\nu(\omega)$ as long as $\mathcal{L}\neq 0$. To obtain a unified approximation over the entire frequency domain, $\nu(\omega)$ is fixed by imposing the exact high- and low-frequency limits of $\bar{C}_{pp}(\omega)$:

$$\lim_{\omega\to 0}\bar{C}_{pp}(\omega)=3m^2D , \tag{3.2}$$

$$\lim_{\omega\to\infty}\bar{C}_{pp}(\omega)\to\langle p^2\rangle(i\omega)^{-1}-Z^2e^2\langle E^2\rangle(i\omega)^{-3} +Z^2e^2\langle\dot{E}^2\rangle(i\omega)^{-5}+\cdots . \tag{3.3}$$

Here $\dot{E}$ is the time derivative of the electric field at $t=0$, and D is the self-diffusion coefficient. For the OCP, $\langle E^2\rangle$ can be calculated exactly,[15]

$$\langle E^2\rangle=4\pi nk_BTZ_0/Z , \tag{3.4}$$

where n is the density and T is the temperature. Also $\langle\dot{E}^2\rangle$ can be calculated from the pair and triplet equilibrium correlation functions[6]

$$\langle\dot{E}^2\rangle=\frac{Zm_0}{Z_0m}\langle E^2\rangle\frac{\omega_p^2}{3}\left[1+\frac{6m}{\mu}\int_0^{\infty}dr\, r^{-4}g^{(2)}(r) +\tfrac{9}{2}\int_0^{\infty}dr\frac{1}{r}\int_0^{\infty}dr'\frac{1}{r'}\int_0^{\pi}d\theta\sin\theta(3\cos^2\theta-1)g^{(3)}(r,r',\hat{\mathbf{r}}\cdot\hat{\mathbf{r}}')\right] . \tag{3.5}$$

Here ω_p is the plasma frequency and μ is the reduced mass. (In practice, the term with $g^{(3)}$ is small compared to the first term on the right-hand side and has been neglected in the calculations of the next two sections.) Finally, the self-diffusion coefficient can be calculated accurately and efficiently from a simple kinetic theory,[16] whose primary input is the radial distribution function $g(r)$. The right-hand sides of Eqs. (3.2) and (3.3) can be taken as known, therefore, even for strongly coupled plasmas. These limits for $\bar{C}_{pp}(\omega)$ can be incorporated by a simple two-parameter representation of $\nu(\omega)$,

$$\nu(\omega)=\nu/(1+i\omega\tau) , \tag{3.6}$$

where ν and τ are constants to be determined from (3.2) and (3.3). This form of $\nu(\omega)$ also satisfies the conditions in (2.12). Use of (3.1) and (3.6) in (3.3) then gives

$$\nu/\tau=\left[\frac{\langle\dot{E}^2\rangle}{\langle E^2\rangle}-\int d\mathbf{p}\int d\varepsilon\,\phi(p)Q(\varepsilon)\frac{(\mathcal{L}^2 p_i)^2}{\langle(Ze\mathbf{E})^2\rangle}\right] \tag{3.7}$$

Also, substitution of (3.1) and (3.6) in (3.2) determines ν in terms of D,

$$\begin{aligned} 3m^2D&=\int d\mathbf{p}\,\phi(p)\mathbf{p}\cdot\Lambda^{-1}(0)\mathbf{p} ,\\ [\nu+\Lambda(0)]^{-1}&=\int d\varepsilon\,Q(\varepsilon)(\nu-\mathcal{L})^{-1} . \end{aligned} \tag{3.8}$$

It is shown in Sec. IV that Eq. (3.8) implies that ν is approximately proportional to the diffusion coefficient D.

The operator $\mathcal{L}$ is defined in terms of a tensor $\sigma_{ij}(\varepsilon)$. If the center-of-mass motion is only weakly dependent on the internal degrees of freedom, then $\sigma_{ij}(\varepsilon)$ has the simple form

$$\begin{aligned} m\sigma_{ij}(\varepsilon)&=Q^{-1}(\varepsilon)\left\langle\delta(\varepsilon-\mathbf{E})\frac{\partial E_j}{\partial r_i}\right\rangle\\ &=n\int d\mathbf{r}\,g^{(2)}(\mathbf{r};\varepsilon)\frac{\partial E_j(r)}{\partial r_i} . \end{aligned} \tag{3.9}$$

Here $g^{(2)}(\mathbf{r};\varepsilon)$ is a generalization of the pair correlation function: the probability density for an ion at position $\mathbf{r}$ relative to the radiator *given* that the field is $\mathbf{E}=\varepsilon$. This quantity can be calculated from an extension of existing methods for the microfield distribution $Q(\varepsilon)$.[17] It may be noted that $\sigma_{ij}(\varepsilon)$ is closely related to $Q(\varepsilon)$ by the stationary condition (2.9). Neglecting dependence on internal degrees of freedom, the latter leads to

$$\frac{\partial\ln Q(\varepsilon)}{\partial\varepsilon}=-\frac{Ze\varepsilon}{mk_BT\sigma(\varepsilon)} , \tag{3.10}$$

where $\sigma(\varepsilon)\equiv\hat{\varepsilon}_i\sigma_{ij}(\varepsilon)\hat{\varepsilon}_j$. The field dependence of $\sigma(\varepsilon)$ is a measure of the deviation of $Q(\varepsilon)$ from a Gaussian distribution.

IV. TRANSPORT PROPERTIES

The basic correlation functions characterizing center-of-mass motion are the momentum autocorrelation function and the dynamical self-structure factor. The calculation of these correlation functions from the model of the Sec. III is straightforward, once the operator $\Lambda(\omega)$ of Eq. (3.1) has been determined. In this section the dependence of correlation functions on internal degrees of freedom is neglected, for comparison with computer simulations of point-charge radiator dynamics. The self-structure factor is determined from the correlation function with $A=B=1$,

$$\begin{aligned} S(\mathbf{k},\omega)&=2\,\mathrm{Re}\bar{C}_{11}(\mathbf{k},\omega)\\ &=2\,\mathrm{Re}\int d\mathbf{p}\,\phi(p)[i\Delta\omega+\Lambda(\Delta\omega)]^{-1} , \end{aligned} \tag{4.1}$$

where now $\Lambda(\Delta\omega)$ is determined from (2.16) with $L(a,\varepsilon)=0$. Although manageable, the calculation of $\Lambda(\Delta\omega)$ is still quite difficult; so we explore the possibility of a further simplification. Since the troublesome component of the model is the operator $\mathcal{L}$, a simpler representation for it is introduced by

$$(X,\mathcal{L}Y)\sim c[(X,\varepsilon)\cdot(\mathbf{p},Y)-(X,\mathbf{p})\cdot(\varepsilon,Y)] . \tag{4.2}$$

The functions X and Y are arbitrary, and the constant c is fixed by

$$(\varepsilon_i,\mathcal{L}p_i)=Ze\langle E^2\rangle=c(\varepsilon_i,\varepsilon)\cdot(\mathbf{p},p_i) , \tag{4.3}$$

or $c=Ze/mk_BT$. The motivation for this approximation is that it incorporates the exact matrix elements of $\mathcal{L}$ with respect to the functions $\mathbf{p}$ and ε, and is consistent with the required properties (2.9). Consequently, all the relationships among correlation functions of the preceding sections are valid with (4.2) as well. For example, the relationship $d\mathbf{p}(t)/dt=e\mathbf{Z}\mathbf{E}(t)$ leads to a corresponding relationship of the momentum and field autocorrelation functions

$$(eZ)^2\bar{C}_{EE}(\omega)=i\omega[\langle p^2\rangle-i\omega\bar{C}_{pp}(\omega)] . \tag{4.4}$$

This equality is preserved by (4.2), as are the limits (3.2) and (3.3).

With this approximate form for $\mathcal{L}$, it is straightforward to determine $\Lambda(\Delta\omega)$. The details are given in Appendix C, with the result

$$\begin{aligned} &\Lambda(\Delta\omega)=\alpha(k,\omega)P ,\\ &\alpha(k,\omega)\equiv\tfrac{1}{3}c^2mk_BT\langle E^2\rangle\int d\mathbf{p}\,\phi(p)[i\Delta\omega+\nu(k,\omega)]^{-1} , \end{aligned} \tag{4.5}$$

where P is the projection operator onto $\mathbf{p}$. The eigenvalues of $\Lambda(\Delta\omega)$ are then simply 0 and $\alpha(k,\omega)$, and the correlation functions are easily calculated. For example, the momentum autocorrelation function is found to be

$$\bar{C}_{pp}(\omega)=3mk_BT[i\omega+\alpha(0,\omega)]^{-1} . \tag{4.6}$$

This result is closely related to an exact continuous fraction representation truncated at fourth order, with parameters determined by the first five frequency moments and the diffusion coefficient. The latter is obtained from (3.2) or (3.8),

$$D=3\nu(k_BT)^2/(Ze)^2\langle E^2\rangle , \tag{4.7}$$

which expresses the precise way in which ν is calculated for the model. Similarly, the approximation (4.2) allows further reductions of expression (3.7) for τ,

$$\nu/\tau=\left[\frac{\langle\dot{E}^2\rangle}{\langle E^2\rangle}-\langle(eZE)^2\rangle/\langle p^2\rangle\right] . \tag{4.8}$$

To test the accuracy of the approximations made to this point it is useful to compare with recent computer simulations of the electric field autocorrelation function. This function is determined directly from Eqs. (4.4) and (4.6),

$$\bar{C}_{EE}(\omega)=\langle E^2\rangle i\omega\{i\omega[i\omega+\nu(0,\omega)] + \tfrac{1}{3}mk_BTc^2\langle E^2\rangle\}^{-1} . \quad (4.9)$$

Figure 1 shows the comparison with the computer simulations for plasma parameters $\Gamma=1$, 2, and 5. The agreement is quite good over the entire frequency range, suggesting that the model is reasonable for calculating transport properties.

The self-structure factor is also easily determined from (4.1) with (4.5). The details are given in Appendix C with the result

$$S^*(k,\omega)\equiv kv_0S(k,\omega) = 2\,\mathrm{Im}[\phi(z)+\Delta(k,z)]/[1-z\Delta(k,z)] , \quad (4.10)$$
$$\Delta(k,z)\equiv\frac{1}{3k^2}\langle(cmE)^2\rangle\phi\left[z+\frac{i\nu}{kv_0}\right][1+z\phi(z)] .$$

Here v_0 is the thermal velocity, $z=-\omega/kv_0$, and $\phi(z)$ is the plasma dispersion function. The corresponding time correlation function is defined by

$$F(k,t)=\int_0^\infty dt\cos(\omega t)S(k,\omega) . \quad (4.11)$$

Computer simulations of Bernu[7] indicate $F(k,t)$ is very well described for all k,t at $\Gamma=1$, 10, and 100 by the Gaussian limit[4]

$$[F(k,t)]_{\text{Gaussian}}\equiv\exp\left[-\frac{k^2}{3m^2}\int_0^t d\tau(t-\tau)C_{pp}(\tau)\right] . \quad (4.12)$$

This approximation expresses the dynamical properties of $S(k,\omega)$ entirely in terms of the momentum autocorrelation function. It is straightforward to verify that the model result (4.10) preserves the exact form of the Gaussian limit. Since the model predicts an accurate momentum correlation function, $S(k,\omega)$ will also be accurate. More detailed results will be presented elsewhere.

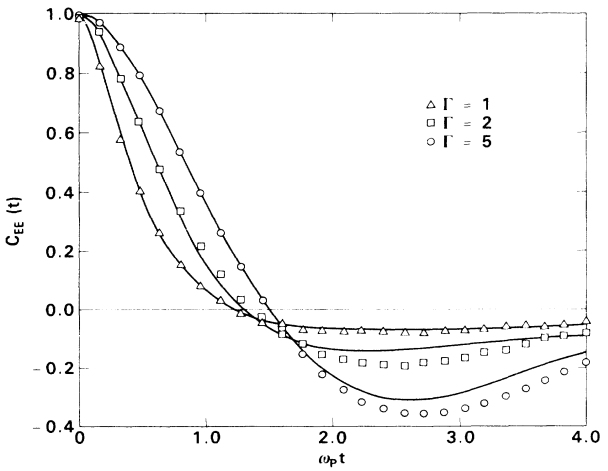

FIG. 1. Electric field autocorrelation function with $Z=Z_0$ for $\Gamma=1$, 2, and 5, from Eq. (4.9) (——) and molecular dynamics (△, □, ○).

V. SPECTRAL LINE SHAPES

Spectral lines emitted from plasmas are broadened by the center-of-mass motion of the radiators, and by the interaction of the radiators with the electrons and ions in the plasma. In the traditional theories of line broadening these three problems (Doppler, ion, and electron broadening) are solved independently of one another. Furthermore, the large mass difference of the electrons and ions leads to very different approaches to estimating their effects on line shapes. It is usual to treat the electron broadening as completely collisional, while the ions are assumed to be stationary during the radiation time. However, there is now strong evidence that this last assumption can lead to substantial errors near the center of intrinsic (non-Doppler-broadened) line profiles. For neutral radiators, the evidence is experimental,[9] and theoretical methods have been developed that adequately describe the effects of ion motion in that case.[1,2,11] For charged radiators the evidence is in the form of numerical simulations.[10,18,19] In this section we will use our model to investigate the effects of ion motion on spectral lines emitted from highly charged, hydrogenic radiators in dense plasmas, and we will compare our results with the recent simulations of Stamm *et al.*[10] In these simulations, the electrons were accounted for through the usual impact approximation, but the ion dynamics were traced in detail. Therefore, the effects of ion motion and Stark-Doppler coupling could be evaluated. The findings indicated that while the effects of ion dynamics were significant, the coupling between the center-of-mass motion and the internal degrees of freedom of the radiator was very weak.

The line-shape function is determined from the dipole autocorrelation function for the radiating ion,[8]

$$I(\omega)=\tfrac{1}{3}\,\mathrm{Re}\bar{C}_{dd}(k,\omega) \equiv\frac{1}{3V}\int_0^\infty dt\,e^{-i\omega t}\langle(\mathbf{d}e^{-i\mathbf{k}\cdot\mathbf{r}})\cdot(\mathbf{d}(t)e^{i\mathbf{k}\cdot\mathbf{r}(t)})\rangle , \quad (5.1)$$

where $k=\omega/c$. Our model can be applied to the problem by using Eqs. (2.13) and (2.14) with both A and B taken to be atomic dipole operator $\mathbf{d}$. The resulting expression describes plasma broadening, Doppler broadening with Dicke narrowing, and their coupling. The correlation between the Doppler and Stark broadening is contained in the operator $\mathcal{L}$. Because this correlation was found to be small in the simulations, we set $\mathcal{L}=0$ in the following discussion. Further justification for this approximation will be made later. Dropping $\mathcal{L}$ simplifies Eq. (5.1) to the familiar convolution of a Doppler profile and a Stark broadened line. The latter is found to be

$$I_p(\omega)=\tfrac{1}{3}\,\mathrm{Re}\,\mathrm{Tr}_a\,\mathbf{d}\cdot f(a)[1-G(\Delta\omega)\nu(\Delta\omega)]^{-1}G(\Delta\omega)\mathbf{d}\ , \tag{5.2}$$

$$G(\Delta\omega)\to\int d\varepsilon\, Q(\varepsilon)R\ ,$$

where R is determined by Eq. (B2) with $\mathcal{L}$ and k set equal to zero, and the electron width operator added to the interaction term,

$$R^{-1}=i[\omega+L(a,\varepsilon=0)]+\nu-L_I(\varepsilon)-\Phi_e\ . \tag{5.3}$$

Further simplification is obtained by focusing attention on a specific line and by making two approximations common in line-broadening theory. We ignore the mixing of states with different principal quantum numbers by the ion field and the broadening of the lower state.[8] With these approximations, L_I may be replaced with $\boldsymbol{\varepsilon}\cdot\mathbf{d}/i\hbar$ and Φ_e by an atomic operator whose matrix elements in spherical states are[20]

$$(n,l,m\mid\Phi_e\mid n,l',m')=\frac{n^2}{4}(n^2-l^2-l-1)\delta_{ll'}\delta_{mm'}\phi\ , \tag{5.4}$$

where $\mid n,l,m)$ represents a state with principal quantum number n and angular numbers l and m, and ϕ depends only on n and the plasma conditions. Furthermore, one finds that the matrix elements of G are (the dependence on n is now suppressed)

$$(l,m\mid G(\Delta\omega)\mid l',m')=\delta_{ll'}\delta_{mm'}\frac{4\pi}{2l+1}\sum_{\bar m=-l}^{l}\int_0^\infty d\varepsilon\,\varepsilon^2Q(\varepsilon)(l,\bar m\mid U\mid l,\bar m)$$

$$\equiv\delta_{ll'}\delta_{mm'}G_l(\Delta\omega)\ , \tag{5.5}$$

where $U=\mathcal{D}R\mathcal{D}^{-1}$ and $\mathcal{D}$ is a rotation that aligns $\boldsymbol{\varepsilon}$ with the z axis. In other words, the matrix elements of U are exactly those appearing in the static theories of line broadening, but with the frequency shift $\Delta\omega$ replaced by $\Delta\omega+i\nu$. For lines in the Lyman series, transitions occur between excited levels with $l=1$ to the ground state, and we find

$$I_p(\omega)=\mid(n,1\mid d\mid 1,0)\mid^2\mathrm{Re}[1-\nu(\Delta\omega)G_1(\Delta\omega)]^{-1}\times G_1(\Delta\omega)\ . \tag{5.6}$$

This is a particularly simple expression, and once ν and τ are determined, it is as easy to evaluate as a static profile.

We have estimated the effects of ion dynamics in the

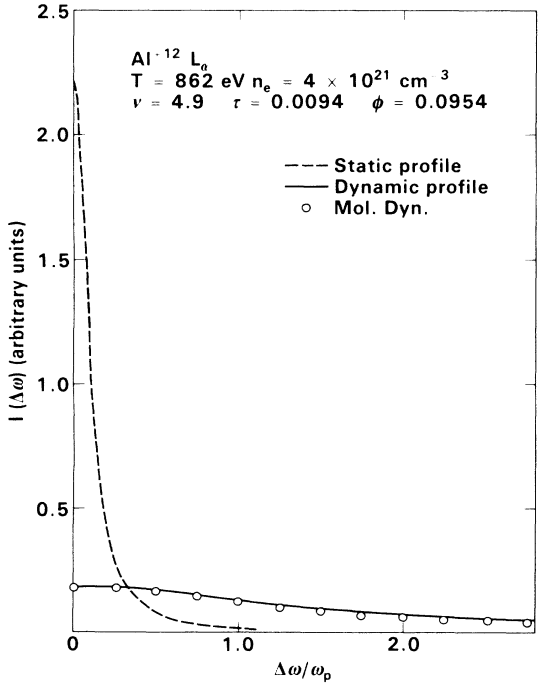

FIG. 2. Lyman-α spectral line shape for Al^{+12} at $T=862$ eV and $n_e=4\times10^{21}$ cm^{-3}, or $\Gamma=0.267$, for the present model (——), molecular dynamics (○,○,○), and for static ions (— — —). Also shown are the constants ν and τ from Eqs. (4.7) and (4.8), and the electron width ϕ of Eq. (5.4).

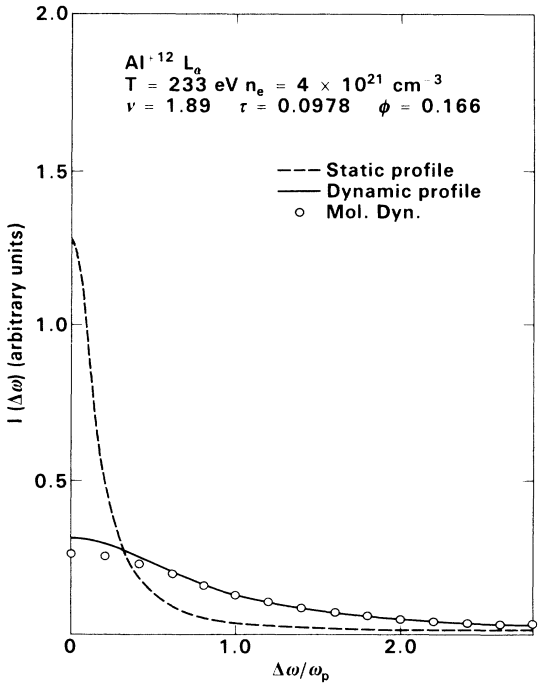

FIG. 3. Same as Fig. 2 at $T=233$ eV and $n_e=4\times10^{21}$ cm^{-3}, or $\Gamma=1.0$.

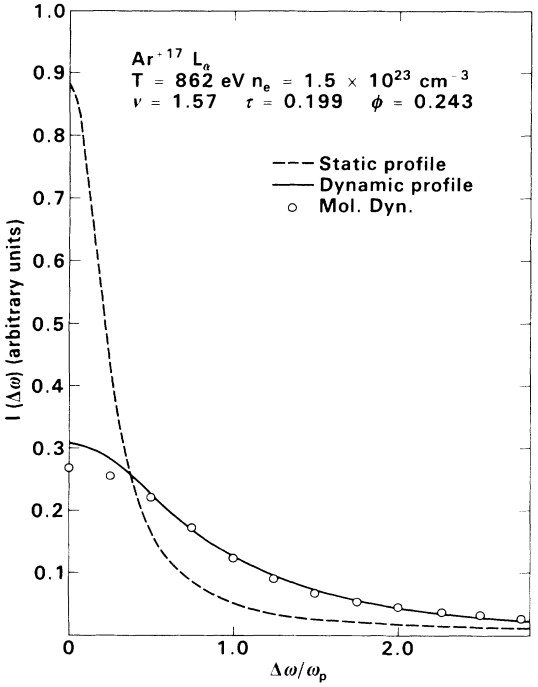

FIG. 4. Same as Fig. 2 for Ar^{+17} at $T=862$ eV and $n_e=1.5\times10^{23}\,cm^{-3}$ or $\Gamma=1.6$.

Al^{+12} and Ar^{+17} plasmas considered in Ref. 10. The results for Lyman α ($n=2$) are illustrated in Figs. 2–4 and for Lyman β ($n=3$) in Figs. 5–7. Calculations were made using Eq. (5.6) directly *and* with the corresponding more complicated expression which results when $\mathcal{L}$ is not neglected. The differences for Lyman α were imperceptible and those for Lyman β were only a few percent. The figures show calculations using the more general expressions, but the small differences further justify the use of Eq. (5.6) alone. The figures also show the quasistatic

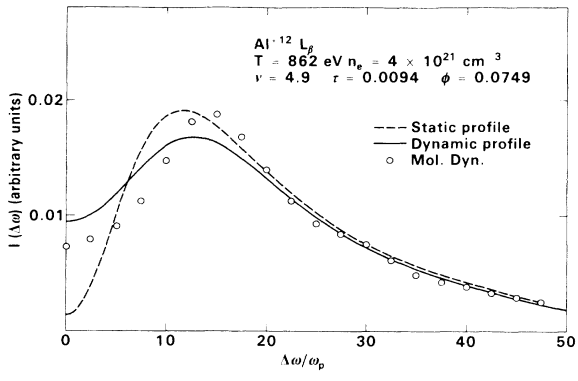

FIG. 5. Lyman-β spectral line shape for same conditions as Fig. 2.

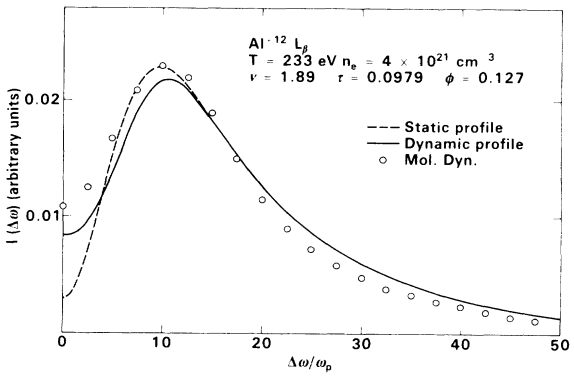

FIG. 6. Lyman-β spectral line shape for same conditions as Fig. 3.

profiles and the simulation results. Ion motion effects are clearly significant at line center for all of the cases considered, and our model is remarkably good for Lyman α and quite reasonable for Lyman β. The microfield distributions used in the quadratures were precisely the ones used in the simulations, and the parameters ν and τ were determined from the methods outlined in Sec. III. The latter may represent a slight discrepancy since the simulations were done for screened ions and the discussion in Sec. III is for an OCP, but because of the large ionic charges the electron screening had a negligible effect on the ion dynamics in the simulations.[21] In addition, a comparison of the self-diffusion for OCP's and systems of screened ions at these conditions shows very small differences. Therefore, we believe the comparison with the simulations is a significant test of our model.

VI. DISCUSSION

Our goal in this paper has been to construct a unified model of both the transport and radiative properties of ions in dense plasmas that is both accurate and simple to

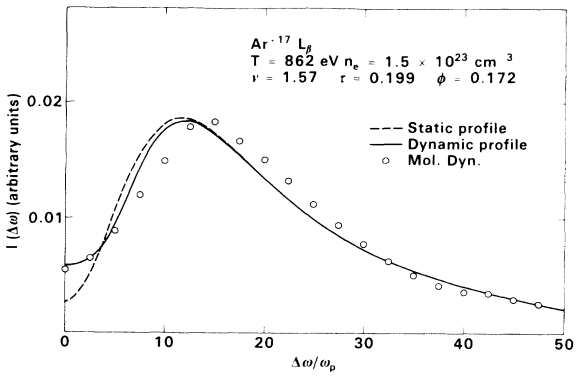

FIG. 7. Lyman-β spectral line shape for same conditions as Fig. 4.

use. Equations (2.13) and (2.14) define such a model based on the assumption that the statistical dynamics of the plasma can be represented by the "kinetic model" of Eq. (2.11). This model preserves the important exact dynamical properties, (2.9) and (2.10), and has a free parameter, $\nu(\Delta\omega)$, that can be chosen to incorporate additional exact limits. Here, we have determined $\nu(\Delta\omega)$ such that the momentum autocorrelation function is asymptotically correct in the high- and low-frequency domains. To explore the validity of the model, one additional approximation was introduced, Eq. (4.2), whereby all calculations could be reduced to quadratures. This second approximation is perhaps the most serious and least controlled. Nevertheless, it describes well the electric field autocorrelation function of Fig. 1, although some discrepancy in the negative region at large plasma parameter is noted. Since the model preserves the proper relationship of the electric field, momentum, and self-structure correlation functions these latter transport properties have a similar accuracy.

The calculation of spectral line shapes has focused on the specific effects of ion motion. The computer simulations suggest large effects near line center, compared to the standard static ion theories, and the model presented here reproduces these effects quite well for Lyman α. It should be stressed that the quantitative features of this ion motion are determined by the self-diffusion coefficient, which appears in the radiative properties as a consequence of the unified treatment with transport properties. Setting $\tau=0$ in all of the above cases leads to insignificant changes in the profile. Hence, very reasonable estimates of ion dynamics effects can be expected from Eq. (5.6) with the only input being the self-diffusion coefficient. The agreement with computer simulations for Lyman β is somewhat less favorable than that for Lyman α. We note that in both cases ion dynamics effects are important only at line center. Since density diagnostics depend upon fitting the wings of the line profiles, we do not expect density measurements to be altered significantly.

Ion motion effects on spectral lines have also been calculated by Cauble and Griem,[11] using a short-time expansion for the electric field dynamics. The limitations of this approach have been noted by Sanchez, Fulton, and Griem[22] in their analysis of low-density spectral lines, as well as by Stamm *et al.*[10] In contrast, our model is constructed by fitting both short- and long- time limits, and is expected to interpolate reasonably between these limits. In general, its combination of simplicity and accuracy makes our model a promising approach to estimating the effects of ion dynamics in dense plasmas.

ACKNOWLEDGMENTS

The authors are indebted to E. L. Pollock for providing the computer simulation data and for helpful suggestions. The research of J.W.D. was supported by National Science Foundation Grant No. CHE-84-11932; the research of D.B.B. and C.A.I. was performed under the auspices of the U.S. Department of Energy by Lawrence Livermore National Laboratory under Contract No. W-7405-Eng-48.

APPENDIX A: PROJECTION OPERATOR METHOD

The explicit form of the correlation function $C_{AB}(t)$ is

$$C_{AB}(t)=V^{-1}\mathrm{Tr}\,A\rho B(t)\ , \tag{A1}$$

where ρ is the equilibrium density matrix and the trace is taken over both ion and plasma states. The variables A and B are taken to be functions of the internal degrees of freedom of the ion, denoted by a, and other degrees of freedom denoted by $\hat{b}$ (the latter represent generically the ion center-of-mass variables and the electric microfield),

$$A=A(a,\hat{b}),\quad B=B(a,\hat{b})\ . \tag{A2}$$

The average in (A1) can be performed in two stages,

$$C_{AB}(t)=\int db\ \mathrm{Tr}_a\, A(a,b)f(a,b)B(a,b;t)\ . \tag{A3}$$

Here, $B(a,b;t)$ represents an average of $B(t)$ over all degrees of freedom except a, for fixed values of $\hat{b}=b$,

$$B(a,b;t)\equiv \mathrm{Tr}'\rho_b B(t)\ , \tag{A4}$$

and ρ_b is the constrained density matrix

$$\rho_b\equiv f^{-1}(a,b)\delta(\hat{b}-b)\rho\ . \tag{A5}$$

Finally, $f(a,b)$ is the reduced density matrix in the subspace of variables, a and $\hat{b}$,

$$f(a,b)\equiv \mathrm{Tr}'\delta(\hat{b}-b)\rho\ . \tag{A6}$$

The prime on the trace denotes a trace with respect to all degrees of freedom except a. Consequently, the form (A3) represents an initial average over the "irrelevant" degrees of freedom, followed by an average over the relevant variables, a and $\hat{b}$. The final average is typically a manageable computational problem since only a relatively few degrees of freedom are involved. The difficult many-body problem is therefore the determination of the first average, $B(a,b;t)$.

The quantity $B(a,b;t)$ can be interpreted as a projection of $B(t)$ into the subspace $a,\hat{b}$,

$$B(a,b;t)=[PB(t)]_{\hat{b}=b}\ . \tag{A7}$$

The projection operator is defined by

$$PX\equiv\int db\ \delta(b-\hat{b})\mathrm{Tr}'\rho_b X\ . \tag{A8}$$

The Heisenberg equations of motion for $B(t)$ are

$$\left[\frac{\partial}{\partial t}-L\right]B(t)=0\ ,\qquad LB=\frac{1}{i\hbar}[B,H]\ , \tag{A9}$$

where H is the Hamiltonian for the system. The equations of motion for $B(a,b;t)$ now follow from the Zwanzig-Mori projection operator method[12]

$$\left[\frac{\partial}{\partial t}+v(b)\frac{\partial}{\partial b}+L(a,\varepsilon)\right]B(a,b;t)=\int_0^t d\tau\, M(t-\tau)B(a,b;\tau)\ , \tag{A10}$$

with the definitions

$$
\begin{aligned}
&v(b)\equiv \mathrm{Tr}'\rho_b(L\hat{b})\ ,\\
&L(a,\varepsilon)X(b)\equiv\frac{1}{i\hbar}[X,(H_a+\boldsymbol{\varepsilon}\cdot\mathbf{d})]\equiv L(a)+L_I(\varepsilon)\ ,\\
&M(t)X(b)\equiv f^{-1}(a,b)\frac{\partial}{\partial b}\int db'\,f(a,b)\mathrm{Tr}'\left[\rho_b(L\hat{b})U(t)(1-P)(L\hat{b})\delta(b'-\hat{b})\frac{\partial}{\partial b'}X(b')\right]\ ,\\
&U(t)\equiv \exp(1-P)L(1-P)t\ .
\end{aligned}
\tag{A11}
$$

Explicit use has been made of the assumption that the coupling of internal degrees of freedom of the ion to the plasma is only through a dipole interaction, $\mathbf{E}\cdot\mathbf{d}$. Also, H_a denotes the Hamiltonian for the isolated atom. More explicitly, substituting $\hat{b}=(\hat{\mathbf{r}},\hat{\mathbf{p}},\hat{\mathbf{E}})$ gives

$$
\begin{aligned}
&\left[\frac{\partial}{\partial t}-\frac{\mathbf{p}}{m}\cdot\nabla-\mathcal{L}-L(a,\varepsilon)\right]B(\mathbf{r},\mathbf{p},\boldsymbol{\varepsilon};t)=\int_0^t d\tau\,M(t-\tau)B(\mathbf{r},\mathbf{p},\boldsymbol{\varepsilon};\tau)\ ,\\
&\mathcal{L}=Ze\boldsymbol{\varepsilon}\cdot\nabla_p+p_i\sigma_{ij}(\varepsilon)\frac{\partial}{\partial\varepsilon_j}\ ,\\
&\sigma_{ij}(\varepsilon)=m^{-1}\mathrm{Tr}'\rho_b\frac{\partial E_j}{\partial\hat{\mathbf{r}}_i}\ .
\end{aligned}
\tag{A12}
$$

Similarly, the operator $M(t)$ becomes

$$
\begin{aligned}
&M(t)X(\mathbf{r},\mathbf{p},\boldsymbol{\varepsilon})=f^{-1}(a,\mathbf{p},\boldsymbol{\varepsilon})\frac{\partial}{\partial\varepsilon_i}\int d\mathbf{r}'\int d\mathbf{p}'\int d\boldsymbol{\varepsilon}'\,f(a,\mathbf{p},\boldsymbol{\varepsilon})K_{ij}(a,\mathbf{r},\mathbf{p},\boldsymbol{\varepsilon};\mathbf{r}',\mathbf{p}',\boldsymbol{\varepsilon}';t)\frac{\partial}{\partial\varepsilon_j'}X(\mathbf{r}',\mathbf{p}',\boldsymbol{\varepsilon}')\\
&K_{ij}(a,\mathbf{r},\mathbf{p},\boldsymbol{\varepsilon};\mathbf{r}',\mathbf{p}',\boldsymbol{\varepsilon}';t)\equiv\mathrm{Tr}'\rho_b(\hat{\mathbf{p}}\cdot\nabla_{\hat{\mathbf{r}}}\hat{E}_i)U_t(1-P)(\hat{\mathbf{p}}\cdot\nabla_{\hat{\mathbf{r}}}\hat{E}_j)\delta(\hat{\mathbf{r}}-\mathbf{r}')\delta(\hat{\mathbf{p}}-\mathbf{p}')\delta(\hat{\mathbf{E}}-\boldsymbol{\varepsilon}')\ .
\end{aligned}
\tag{A13}
$$

The relevant properties of M and $\mathcal{L}$ are now readily verified. First, the explicit derivatives with respect to ε_i and ε_j' lead directly to the result

$$
(X,MY)=0=(Y,MX) \tag{A14}
$$

for X arbitrary and Y independent of $\boldsymbol{\varepsilon}$. Similarly, it follows directly from (A12) that

$$
\begin{aligned}
&\mathcal{L}p_i=Ze\varepsilon_i\ ,\\
&\mathcal{L}\varepsilon_i=p_j\sigma_{ji}(\boldsymbol{\varepsilon})\ .
\end{aligned}
\tag{A15}
$$

Finally, since $p_i\sigma_{ij}(\boldsymbol{\varepsilon})=m^{-1}\mathrm{Tr}'\rho_b LE_j$,

$$
\begin{aligned}
(X,(\mathcal{L}+L_a)Y)&=\mathop{\mathrm{Tr}}_a\int d\boldsymbol{\varepsilon}\int d\mathbf{p}\,X^{\dagger}(a,\boldsymbol{\varepsilon},\mathbf{p})f(a,\boldsymbol{\varepsilon},\mathbf{p})\\
&\quad\times[\mathcal{L}+L(a,\boldsymbol{\varepsilon})]Y(a,\boldsymbol{\varepsilon},\mathbf{p})\\
&=-([\mathcal{L}+L(a,\boldsymbol{\varepsilon})]X,Y)\\
&\quad-\mathop{\mathrm{Tr}}_a\int d\boldsymbol{\varepsilon}\int d\mathbf{p}\,X^{\dagger}\{[\mathcal{L}+L(a,\boldsymbol{\varepsilon})]f\}Y\ .
\end{aligned}
\tag{A16}
$$

The last term on the right-hand side vanishes since

$$
\begin{aligned}
[\mathcal{L}+L(a,\boldsymbol{\varepsilon})]f(a,b)&=\mathrm{Tr}'\left[L(a,\boldsymbol{\varepsilon})\rho\delta(\hat{b}-b)+\rho\frac{\partial}{\partial b}\delta(\hat{b}-b)L\hat{b}\right]\\
&=\mathrm{Tr}'\{[L(a,\boldsymbol{\varepsilon})\rho]\delta(\hat{b}-b)-\rho[L-L(a,\boldsymbol{\varepsilon})]\delta(\hat{b}-b)\}\\
&=\mathrm{Tr}'(L\rho)\delta(\hat{b}-b)\ ,
\end{aligned}
\tag{A17}
$$

which is zero from stationarity of ρ. Consequently the two properties used in the text are verified:

$$
\begin{aligned}
&(X,[\mathcal{L}+L(a,\boldsymbol{\varepsilon})]Y)=-([\mathcal{L}+L(a,\boldsymbol{\varepsilon})]X,Y)\ ,\\
&[\mathcal{L}+L(a,\boldsymbol{\varepsilon})]f(a,b)=0\ .
\end{aligned}
$$

Finally, Fourier-Laplace transformation of Eq. (A12) yields Eq. (2.8) used in the text.

APPENDIX B: CORRELATION FUNCTIONS

The Laplace transform $\bar{C}_{AB}(\mathbf{k},\omega)$ is obtained from Eq. (2.8),

$$
\begin{aligned}
&\bar{C}_{AB}(\mathbf{k},\omega)=(A,\mathcal{R}B)\ ,\\
&\mathcal{R}^{-1}\equiv i\,\Delta\omega-L_I(\varepsilon)-\mathcal{L}-\bar{M}\ .
\end{aligned}
\tag{B1}
$$

Substitution of the model for $\overline{M}$, Eq. (2.11), gives

$$\mathcal{R}B = RB + R\nu(\Delta\omega)\langle \mathcal{R}B \rangle_\varepsilon ,$$
$$\langle \mathcal{R}B \rangle_\varepsilon \equiv \int d\varepsilon\, Q(\varepsilon) B , \tag{B2}$$
$$R^{-1} \equiv i\,\Delta\omega + \nu(\Delta\omega) - L_I(\varepsilon) - \mathcal{L} .$$

Averaging $\mathcal{R}B$ over $Q(\varepsilon)$ in the first of Eqs. (B2) gives

$$\langle \mathcal{R}B \rangle_\varepsilon = [1 - \langle R \rangle_\varepsilon \nu(\Delta\omega)]^{-1} \langle RB \rangle_\varepsilon . \tag{B3}$$

Substitution of (B2) and (B3) into (B1) gives

$$\overline{C}_{AB}(\omega) = (A, RB) + (A, R\nu(\Delta\omega)[1 - \langle R \rangle_\varepsilon \nu(\Delta\omega)]^{-1} \langle RB \rangle_\varepsilon) . \tag{B4}$$

This is the desired general result, showing that the correlation functions can be computed entirely from the properties of R. While such calculations are still quite complex, the many-body aspects have been removed. For example, the most difficult part of R is the operator $\mathcal{L}$, which defines a six-dimensional first-order partial differential equation.

Further simplifications of (B4) are possible in special cases. First, if there is no dependence of A and B on the electric field, then

$$\overline{C}_{AB} = \operatorname*{Tr}_a \int d\mathbf{p}\, A(a,\mathbf{p}) f(a) \phi(p) \times [i\,\Delta\omega + \Lambda(\Delta\omega)]^{-1} B(a,\mathbf{p}) , \tag{B5}$$

where $f(a)$ is the reduced density operator for the atom,

$$f(a) \equiv \mathrm{Tr}' \rho , \tag{B6}$$

and $\Lambda(\Delta\omega)$ is an operator defined by

$$[i\,\Delta\omega + \nu(\Delta\omega) + \Lambda(\Delta\omega)]^{-1} \equiv \langle R \rangle_\varepsilon \equiv G(\Delta\omega) . \tag{B7}$$

This verifies the results (2.13)–(2.16).

APPENDIX C: APPROXIMATE EVALUATION OF $\Lambda(\mathbf{k},\omega)$

The general definition of Λ for the case of no internal degrees of freedom is given by Eq. (B7), with $L(a,\varepsilon)=0$,

$$[i\,\Delta\omega + \nu(k,\omega) + \Lambda(\Delta\omega)]^{-1} = \int d\varepsilon\, Q(\varepsilon) R(\mathbf{k},\mathbf{p}) ,$$
$$R(\mathbf{k},\mathbf{p}) \equiv [i\,\Delta\omega + \nu(k,\omega) - \mathcal{L}]^{-1} . \tag{C1}$$

Let $X(\mathbf{p})$ and $Y(\mathbf{p})$ be arbitrary functions of $\mathbf{p}$, and consider (X,RY) with the identity

$$R = R_0 + R\mathcal{L}R_0, \quad R_0 \equiv [i\,\Delta\omega + \nu(\Delta\omega)]^{-1} . \tag{C2}$$

Then (X,RY) can be written

$$(X,RY) = (X,R_0Y) + (X,R\mathcal{L}R_0Y) = (X,R_0Y) + c(X,R\varepsilon_i)(p_i,R_0Y) , \tag{C3}$$

where the approximation (4.2) for $\mathcal{L}$ has been used in the second equality, with the fact that $(\varepsilon_i,R_0Y)=0$ for $Y=Y(\mathbf{p})$. Application of (C2) one more time in (C3) gives

$$(X,RY) = (X,R_0Y) - c^2(X,Rp_j)(\varepsilon_j,R_0\varepsilon_i)(p_i,R_0Y) = (X,(1+R_0P\alpha)^{-1}R_0Y) = (X,(R_0^{-1}+\alpha P)^{-1}Y) . \tag{C4}$$

Here P is the projection operator onto $\mathbf{p}$,

$$PX \equiv (mk_BT)^{-1} p_i (p_i,X) \tag{C5}$$

and $\alpha(\mathbf{k},\omega)$ is defined by

$$\alpha(k,\omega) \equiv \tfrac{1}{3}c^2 mk_BT(\varepsilon_i,R_0\varepsilon_i) = \tfrac{1}{3}c^2 mk_BT\langle E^2 \rangle \int d\mathbf{p}\,\phi(p)[i\,\Delta\omega + \nu(k,\omega)]^{-1} . \tag{C6}$$

Equations (C1) and (C4) now give

$$(X,(R_0^{-1}+\Lambda)Y) = (X,(R_0^{-1}+\alpha P)Y) .$$

Since this must hold for all X and Y (independent of ε) the operator Λ can be identified as

$$\Lambda(\Delta\omega) = \alpha(\Delta\omega)P . \tag{C7}$$

The eigenvalues of Λ are 0 and $\alpha(k,\omega)$. This is a particularly simple result, from which the correlation functions are easily obtained. For the case of A and B independent of ε *and* internal variables,

$$\overline{C}_{AB} = \overline{C}^{(0)}_{AB} - \frac{\alpha}{mk_BT}\overline{C}^{(0)}_{Ap_i}\overline{C}_{p_iB} ,$$
$$C^{(0)}_{AB} \equiv \lim_{\eta\to 0+} \int d\mathbf{p}\,\phi(p) A^\dagger(\mathbf{p})(i\,\Delta\omega + \eta)^{-1} B(\mathbf{p}) . \tag{C8}$$

The momentum autocorrelation function and self-structure factors are special cases of (C8),

$$\overline{C}_{pp}(\omega) \equiv \overline{C}_{p_ip_i}(k=0,\omega) = 3mk_BT[i\omega + \alpha(k=0,\omega)]^{-1} , \tag{C9}$$

$$\overline{C}_{11}(k,\omega) = \left[\overline{C}^{(0)}_{11} + \frac{\alpha}{mk_BT}[\overline{C}^{(0)}_{11}\hat{k}_i\hat{k}_j\overline{C}^{(0)}_{p_ip_j} - (\hat{k}_i\overline{C}^{(0)}_{p_i1})^2]\right]\left[1 + \frac{\alpha}{mk_BT}\hat{k}_i\hat{k}_j\overline{C}^{(0)}_{p_ip_j}\right]^{-1} , \tag{C10}$$

$$S(k,\omega) = 2\,\mathrm{Re}\overline{C}_{11}(k,\omega) . \tag{C11}$$

The functions $\bar{C}^{(0)}_{AB}$ can be expressed in terms of the complex plasma dispersion function. For example,

$$\bar{C}^{(0)}_{11}(k,\omega) = -i\phi(z)/kv_0 ,$$
$$\bar{C}^{(0)}_{p_i 1}(k,\omega) = -ik_i m[1+z\phi(z)]/k^2 ,$$
$$k_i k_j \bar{C}^{(0)}_{p_i p_j}(k,\omega) = -ikv_0 m^2 z[1+z\phi(z)] , \tag{C12}$$
$$\alpha(k,\omega) = \frac{-ic^2 m k_B T\langle E^2\rangle}{3kv_0}\phi(z+i\nu(k,\omega)/kv_0) ,$$
$$\phi(z) \equiv \lim_{\eta\to 0+}\int_{-\infty}^{\infty}\frac{dv}{\sqrt{\pi}}\frac{e^{-v^2}}{v-z-i\eta} ,$$

with $z \equiv -\omega/kv_0$ and $v_0^2 \equiv 2/\beta m$. Use of (C12) then gives

$$ikv_0\bar{C}_{11}(k,\omega) = [\phi(z)+\Delta(z)]/[1-z\Delta(k,z)] ,$$
$$\Delta(k,z) \equiv \frac{1}{3k^2}\langle (cmE)^2\rangle\phi(z+i\nu/kv_0)[1+z\phi(z)] , \tag{C13}$$

which is in a form suitable for numerical evaluation.

[1] A. Brissaud and U. Frisch, J. Quant. Spectrosc. Radiat. Transfer **11**, 1767 (1971); J. Math. Phys. **15**, 524 (1974).

[2] J. Seidel, Z. Naturforsch. **32a**, 1195 (1977).

[3] J. Dufty, in *Spectral Line Shapes*, edited by B. Wende (de Gruyter, New York, 1981).

[4] J.-P. Hansen and I. McDonald, *Theory of Simple Liquids* (Academic, New York, 1976); J. P. Boon and S. Yip, *Molecular Hydrodynamics* (McGraw-Hill, New York, 1980).

[5] For a recent overview, see *Radiative Properties of Hot Dense Matter*, edited by J. Davis *et al.* (World-Scientific, Singapore, 1985).

[6] E. L. Pollock and J. C. Weisheit, in *Spectral Line Shapes III*, edited by F. Rostas (de Gruyter, New York, 1985).

[7] B. Bernu, J. Stat. Phys. **21**, 447 (1979).

[8] H. R. Griem, *Spectral Line Broadening by Plasmas* (Academic, New York, 1974).

[9] J. Seidel, in *Spectral Line Shapes*, edited by B. Wende (de Gruyter, New York 1981); M. Geisler, K. Grutzmacher, and B. Wende, in *Spectral Line Shapes III*, edited by F. Rostas (de Gruyter, New York, 1985).

[10] R. Stamm, B. Talin, E. Pollock, and C. Iglesias, Phys. Rev. A **34**, 4144 (1986).

[11] R. Cauble and H. R. Griem, Phys. Rev. A **30**, 3187 (1983).

[12] R. Zwanzig, Phys. Rev. **124**, 983 (1961).

[13] L. Groome, M. Lindenfeld, and J. Dufty, Phys. Rev. A **19**, 304 (1979).

[14] This is analogous to a good model of the linearized Boltzmann operator (the BGK model). See, for example, C. Cercignani, *Theory and Application of the Boltzmann Equation* (Elsevier, New York, 1975), p. 95.

[15] C. Iglesias, J. Lebowitz, and D. MacGowan, Phys. Rev. A **28**, 1667 (1983).

[16] D. B. Boercker, in *Strongly Coupled Plasma Physics*, edited by F. J. Rogers and H. E. DeWitt (Plenum, New York, 1987); D. B. Boercker and E. L. Pollock, Phys. Rev. A **36**, 1779 (1987).

[17] F. Lado and J. Dufty, Phys. Rev. A **36**, 2333 (1987).

[18] R. Stamm, Y. Botzanowski, V. P. Kaftandjian, B. Talin, and E. W. Smith, Phys. Rev. Lett. **52**, 2217 (1984); **54**, 2170 (1985).

[19] R. L. Greene, J. Phys. B **15**, 1831 (1982); D. H. Oza, R. L. Greene, and D. E. Kelleher, Phys. Rev. A **34**, 4519 (1986).

[20] H. R. Griem, M. Blaha, and P. C. Kepple, Phys. Rev. A **19**, 2421 (1979).

[21] E. L. Pollock (private communication).

[22] A. Sanchez, R. D. Fulton, and H. Griem, Phys. Rev. A **35**, 2596 (1987).